

Plasmonic Nanopillar Arrays for Optical Trapping, Biosensing, and Spectroscopy

Arif E. Çetin^a, Ahmet Ali Yanik^a, Cihan Yilmaz^b, Sivasubramanian Somu^b,
Ahmed Busnaina^b and Hatice Altug^a

^aDepartment of Electrical and Computer Engineering, and Photonics Center, Boston University, Boston, Massachusetts 02215, USA

^bNSF Nanoscale Science and Engineering Center for High-rate Nanomanufacturing, Northeastern University, Boston, Massachusetts 02215, USA

ABSTRACT

In this work, we propose a unique plasmonic substrate that combine the strength of localized and extended surface plasmons for optical trapping, spectroscopy and biosensing, all in the same platform. The system is based on periodic arrays of gold nanopillars fabricated on a thin gold sheet. The proposed periodic structure exhibits high refractive index sensitivities, as large as 675 nm/RIU which is highly desirable for biosensing applications. The spectrally sharp resonances, we determine a figure of merit, as large as 112.5. The nanopillar array also supports easily accessible high near-field enhancements, as large as 10.000 times, for surface enhanced spectroscopy. The plasmonic hot spots with high intensity enhancement lead to large gradient forces, 350 pN/W/ μm^2 , needed for optical trapping applications.

Keywords: plasmonics, optical trapping, biosensing, spectroscopy

1. INTRODUCTION

Confinement of light through propagating and extended surface plasmons (SPs) has received significant attention from the fields of biosensing [1], spectroscopy [2] and optical trapping [3]. The development of the plasmonic biosensors is important for wide range of fields from public health to pharmacology. Although these structures show enhanced properties for screening of biological assays, there are major challenges that they face. Most of biosensing platforms are based on the resonance shift method which depends on the refractive index change due to the accumulated biomass on the sensor surface. However, this resonance may also be triggered by the biosamples in the solution which may lead to false positive. We can mitigate this problem by adding a surface enhanced vibrational spectroscopy which can give more specific information of the binding molecule on the sensor surface. The other problem is related to the delivery of the analytes to the sensor surface. This can be achieved by utilizing large optical forces to pull the biosamples to the sensor surface.

In this work, we propose a plasmonic structure for high performance biosensing, spectroscopy and optical trapping at the same time. The system is based on periodic arrays of nanopillars fabricated on a single metal sheet on a supporting dielectric layer as illustrated in Fig.1(a). Fig.1(b) shows the scanning electron microscope (SEM) image of the preliminary fabricated structure. With our proposed structure, we achieve high refractive index sensitivities, $RIS = 675$ nm/RIU with large figure of merits, $FOM = 112.5$ for enhanced biosensing applications. The system supports high near-field intensity enhancements, around 10.000 times, from the plasmonic hot spots whose location depends on the polarization of the illumination light source. This property is highly suitable for spectroscopy applications. These hot spots also enable large optical forces, 350 pN/W/ μm^2 , which is highly desirable for optical trapping/manipulation applications. Our platform, enabling optical trapping of bioparticles, spectroscopy and biodetection at the same time, could find wide range of applications in enhanced biosensing applications.

Further author information: (Send correspondence to H.A.)
H.A.: E-mail: altug@bu.edu, Telephone: 1 (617) 358-4769

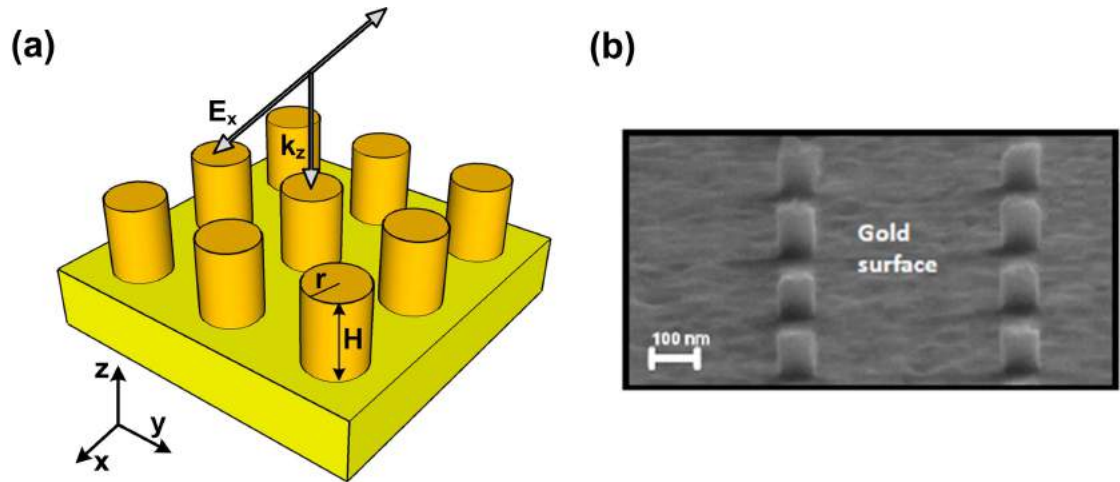


Figure 1. (a) Schematic view of the plasmonic nanopillar array. (b) SEM image of the fabricated nanopillar array with the corresponding parameters: $r = 50$ nm, $H = 100$ nm and $P = 500$ nm.

2. NANOPILLAR ANTENNA RESPONSE

We optimize the structures with 3-dimensional finite-difference-time-domain (3D-FDTD) method by varying the height and radius of the nanopillar, H and r and the periodicity of the array, P . In particular, we find that the structure with $H = 400$ nm, $r = 100$ nm and $P = 600$ nm gives the sharpest spectral behavior as shown in Fig.2(a). It is also interesting to note that, the proposed nanopillar system is perpendicularly illuminated so that this collinear arrangement enables this sharp resonance behavior with minimal alignment requirements.

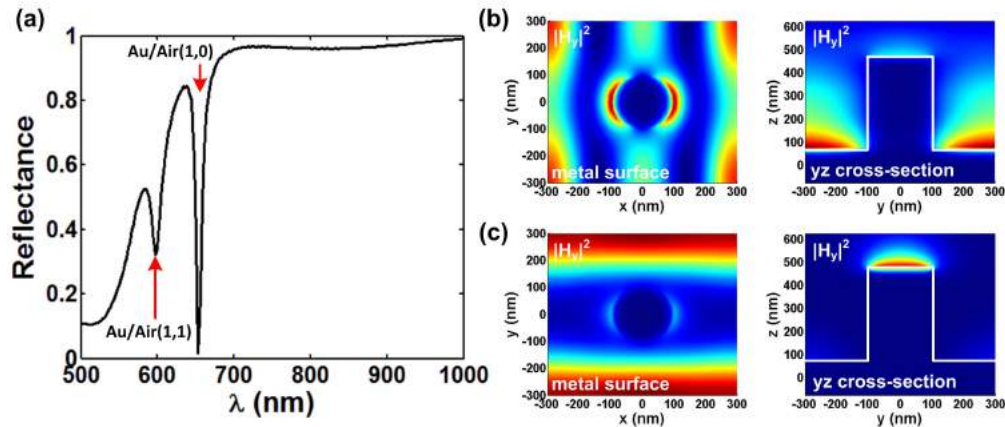


Figure 2. (a) The reflection data for the nanopillar arrays. The intensity distribution of the y -component of the magnetic field, $|H_y|^2$, on the metal surface and through the yz -cross section for (b) SP(1,1) and (c) SP(1,0) modes. The corresponding parameters are $r = 100$ nm, $H = 400$ nm and $P = 600$ nm.

For the periodic arrays, we observe that the structure supports two distinct resonances which correspond to the excitation of the SP modes by different grating orders. To understand the physical origin of these modes, we obtain their near-field profiles at the air-metal interface as well as through the cross section. The weaker resonance dip observed at the shorter wavelengths is due to the SP(1,1) mode. Fig.2(b) shows that at the interface, the structure supports diagonal standing wave pattern in the square lattice. In cross-section, we observe the evanescent decay of the plasmonic field from the surface. The sharper and stronger resonance dip

observed at longer wavelengths is due to the SP(1,0) mode. Fig.2(c) shows that the field distribution shows standing wave pattern along the y-direction. At the cross-section, the array supports a tightly localized field at the top surface of the nanopillar. For our analysis, we focus on SP(1,0) mode, since it gives the sharpest resonance dip.

3. HIGH SENSITIVITIES FOR ADVANCED BIO-SENSING

A highly sensitive nature on the surface conditions is needed for biosensing applications. Fig.3 shows the shift in the resonance dip for different solutions with a refractive index, n . We obtain the refractive index sensitivities as large as, $RIS = 675nm/RIU$ which is a highly desired value for the biosensing applications. With spectrally sharp resonances, we calculate the figure of merit as 112.5.

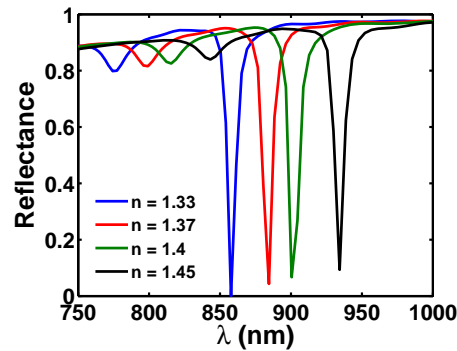


Figure 3. The reflection data for the nanopillar arrays embedded in solutions with different refractive indices, n . The corresponding parameters are $r = 100$ nm, $H = 400$ nm and $P = 600$ nm.

4. HIGH FIELD ENHANCEMENTS FOR SURFACE ENHANCED SPECTROSCOPY

For surface enhanced spectroscopy, large field enhancements are critical. Fig.4 shows the total electric field distribution for SP(1,0) mode at de-ionized (DI) water ($n = 1.33$). Cross-sectional field profile demonstrates that the plasmonic excitations lead to tight field localization around the rims of the nanopillar structure at the top surface with an enhancement factor of 10,000. More interestingly, this strong near-field intensities extend into the surrounding medium. This easily accessible high field enhancement is highly advantageous for vibrational spectroscopy applications since we have the maximum overlap between the biomolecule and the optical field.

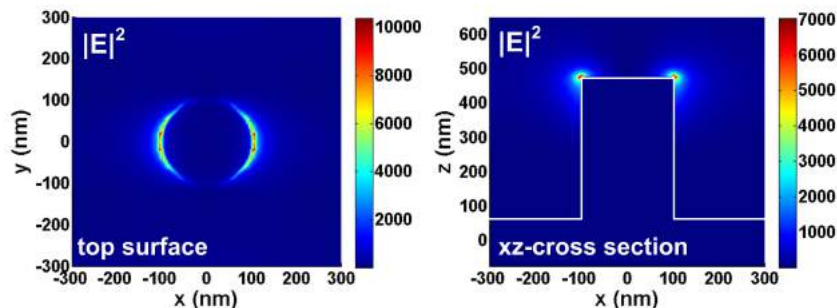


Figure 4. Near-field intensity distribution (total electric field, $|E|^2$) of the nanopillar system embedded in DI water. The corresponding parameters are $r = 100$ nm, $H = 400$ nm and $P = 600$ nm.

5. STRONG OPTICAL FORCES FOR BIOMOLECULE MANIPULATION

The strong localization of SPs at the rims of the nanopillar also allows large optical forces in the vicinity of the antenna. Optical forces depend on the field intensities as well as their gradients. Fig.5(a) shows the electric field intensity at the top surface of the nanopillar. We observe that the structure supports high near field enhancement at two plasmonic hot spots along the polarization direction. These hot spots enhance the near-field intensity up to 10,000 times. We also determine the field intensity profile along the x-direction at the top surface of the nanopillar where the structure is merged in DI water. We observe that this high field intensity drops to zero in a distance less than 100 nm as in Fig.5(b). Hence, nanopillar structures supporting large field intensities that drop sharply are ideal for creating large optical forces for optical trapping/manipulation applications.

For illustration, we calculate the optical forces acting on a dielectric spherical bead with a radius of 50 nm. The refractive index of the bead is $n = 1.4$. The bead is located at the xz-plane and the actual distance between the bead and the top surface of the nanopillar along the x and z directions is 50 nm as shown in Fig.5(c). We calculate the optical forces by integrating the Maxwell stress tensor (MST) over the volume surrounding the bead as shown in Eq.1.

$$F = \oint_S \sum_j \frac{1}{2} \text{Re}(T_{ij} \hat{n}_j) \quad (1)$$

where \hat{n} is the unit vector normal to the surface S and each element of MST is given by

$$T_{ij} = \epsilon E_i E_j^* + \mu H_i H_j^* - \frac{1}{2} \delta_{ij} (\epsilon |\vec{E}|^2 + \mu |\vec{H}|^2) \quad (2)$$

We observe that the structure supports the largest optical force at the spectral resonance dip where almost all of the incident light is coupled to SPs as shown in Fig.5(d). At this resonance wavelength, we calculate the optical force, as large as $350 \text{ pN/W}/\mu\text{m}^2$ which is a quite high value for optical trapping applications.

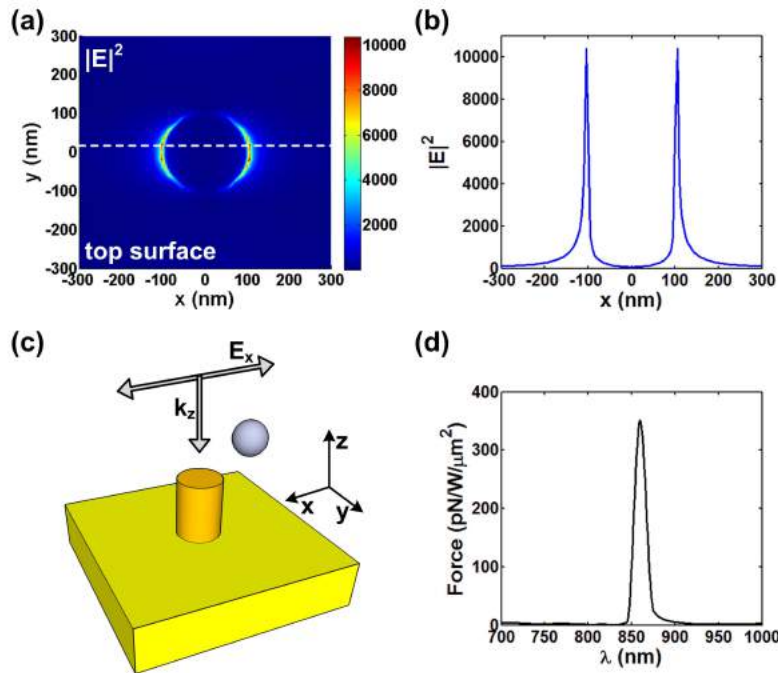


Figure 5. (a) Electric field intensity distribution at the top surface of the nanopillar for SP(1,0) mode where the system is merged in DI water. (b) The field profile determined along the x direction. (The data location is illustrated with a white dashed line in Fig.5(a).) (c) Illustration of the nanopillar structure and the dielectric bead. (d) Calculated optical force vs wavelength. The corresponding parameters are: $r = 100 \text{ nm}$, $H = 400 \text{ nm}$ and $P = 600 \text{ nm}$.

As indicated by the near-field analysis in Fig.4, the near-field gradients are symmetric along the x-direction when the nanopillar array is illuminated by an x-polarized light source. Hence, we expect the largest optical force along the x-direction. To illustrate this, we calculate the forces exerted on the same spherical bead with a radius of 50 nm at three different locations. Fig.6(a) shows the 3-dimensional illustration of the bead in three different locations. For all configurations, the center-to-center distance between the top surface of the nanopillar and the bead is 200 nm so that the actual distance between them is 50 nm. Consequently, the locations are, (i) bead is located on the x-axis (black colored), (ii) bead is located on the diagonal of the xy-axes (red colored), and (iii) bead is located on the y-axis (blue colored). Fig.6(b) shows that the black bead which is along the polarization direction and as a result, closest to the plasmonic hot spots, experiences the largest force.

Our previous calculations show that the hot spot location is along the polarization direction and nanopillar arrays exerts the maximum force from these hot spots due to the high intensity gradient. Therefore, the ability to control the hot spot location thus the amount of the optical force by the polarization variation can be used to manipulate the biomolecules near the biosensor surface. As illustrated in Fig.6(c), changing the polarization direction, we can vary the position of the plasmonic hot spots. As an illustration, in Fig.6(d), for the incident source with an polarization angle, $\theta = 45^\circ$, the hot spots are along the xy-diagonal. Hence, this polarization tuning can be used to orient the biomolecules with respect to the hot spot location so that we can maximize our biosensing and spectroscopy signals.

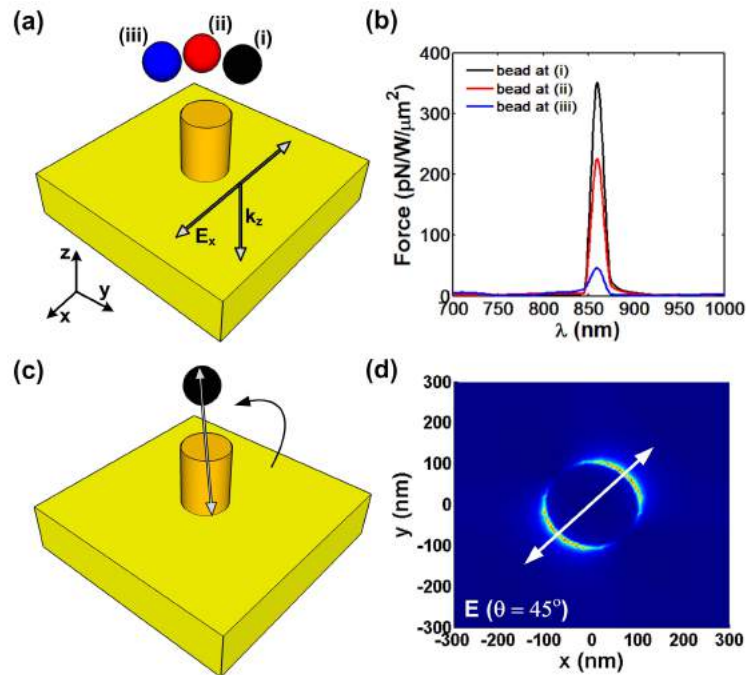


Figure 6. (a) 3-dimensional schematic view of the structure with a bead positioned in three different locations. (b) The optical force exerted on the bead in three different locations. (c) The illustration of the bead manipulation by the polarization direction control. (d) Electric field intensity distribution at the top surface of the nanopillar for the incident wave with the polarization angle of 45° . The corresponding parameters are: $r = 100$ nm, $H = 400$ nm and $P = 600$ nm.

6. FABRICATION OF NANOPILLAR ANTENNAS

In this section, we discuss our experimental effort to the fabricate nanopillar structures. In plasmonics field, lift-off method is commonly used to fabricate nanoparticles. In this fabrication technique, electron beam lithography (EBL) is performed to the surface coated with an e-beam resist and then, the surface is covered with a metal. Here, the lift-off process is performed to remove the metal on the unexposed surfaces. In order to successfully lift off the metal, the height of the resist should be 2-3 times thicker than the height of the deposited metal. For our

proposed structure with a pillar height, 400 nm, we need to use, 1 μm or even thicker e-beam resist. However, to work with such a thick e-beam resist is not practical.

Here, to overcome this limitation, we propose a new fabrication method which is highly desirable for fabrication of tall nanoparticles as illustrated in Fig.7. The fabrication method is lift-off free. In the fabrication process, which is an the assembly process, first, nanoscale vias are fabricated with EBL. Then, 5 nm sized metallic nanoparticles suspended in DI water are precisely assembled into the vias by applying an electric field between top and bottom electrodes. During the assembly process, nanoparticles are fused with the current passing through them resulting in nanopillar formation in the vias. In our fabrication technique, the size of the vias controls the dimension of nanopillars. Since, we use no lift-off process, we can exploit the full thickness of the resist and fabricate tall pillars relatively easily. Fig.1(b) shows the preliminary fabricated nanopillar array with $r = 50$ nm, $H = 100$ nm, and $P = 500$ nm and now we are working on the optimization of the fabrication process to realize proposed structure.

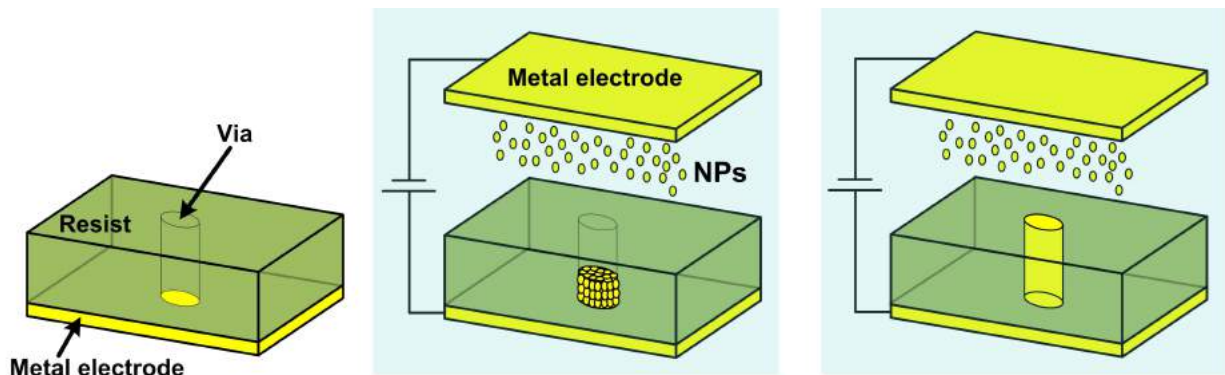


Figure 7. Fabrication process of the nanopillar arrays.

7. CONCLUSION

In conclusion, we propose a plasmonic nanopillar system that merges multiple sensor modalities by using localized and propagating SPs together. The light coupling through a perpendicularly illuminated light source could be advantageous. The system provides high refractive index sensitivities, 675 nm/RIU, with large figure of merits, 112.5 which is highly desirable for biosensing applications. In addition, easily accessible high field enhancements, around 10,000 times, can be advantageous for surface enhanced spectroscopy applications. Strong optical forces exerted from the plasmonic hot spots, $350 \text{ pN/W}/\mu\text{m}^2$, can be controlled by the polarization direction of the illumination source. Combining sensing and spectroscopy can mitigate the problems associated with unspecific bindings leading to false positive while the strong optical forces can be used to trap and manipulate biomolecules near the sensor surface. Our proposed system, integrating biosensing, spectroscopy and optical trapping all in the same platform, could find wide range of applications.

ACKNOWLEDGMENTS

This work is supported by National Science Foundation CAREER Award (ECCS-0954790) Engineering Research Center on Smart Lighting (EEC-0812056), NSF Grant No. 0832785, as well as by ONR Young Investigator Award, Massachusetts Life Science Center New Investigator Award. Authors acknowledge Kostas Research Center at Northeastern University and Boston University Photonics Center.

REFERENCES

1. A. V. Kabashin, P. Evans, S. Pastkovsky, W. Hendren, G. A. Wurtz, R. Atkinson, R. Pollard, V. A. Podolskiy and A. V. Zayats, "Plasmonic nanorod metamaterials for biosensing," *Nature Mater.* **8**, pp. 867 - 871, 2009.

2. Z. Huang, G. Meng, Q. Huang, Y. Yang, C. Zhu and C. Tang, "Improved SERS performance from Au nanopillar arrays by abridging the pillar tip spacing by Ag sputtering," *Adv. Mater.* **22**, pp. 4136 - 4139, 2010.
3. V. D. Miljkovic, T. Pakizeh, B. Sepulveda, P. Johansson, and M. Kall, "Optical forces in plasmonic nanoparticle dimers," *Phys. Chem. C* **114**, pp. 7472 - 7479, 2010.